LAPPEENRANTA UNIVERSITY OF TECHNOLOGY
DEPARTMENT OF ELECTRICAL ENGINEERING

Oxygen adsorption on clean and oxygen precovered Cu(100)

The subject of this thesis was approved in the council of the Department of Electrical Engineering at 5.4.2004.

The supervisor of this study was professor Matti Alatalo and the examiner was PhD Adam Foster.

Lappeenranta 20.4.2004

Antti Puisto
Korpisuonkatu 16 C 33
53 850 Lappeenranta
tel. 050-3497962

ABSTRACT

Author:	Puisto, Antti
Subject:	**Oxygen adsorption on clean and O precovered Cu(100)**
Department:	Department of Electrical Engineering
Year:	2004
Place:	Lappeenranta

Master's thesis. Lappeenranta University of Technology. 49 pages and 35 figures.

Supervisor:	Professor Matti Alatalo
Keywords:	Oxygen, oxidation, copper, Cu, O, adsorption

The early stages of the oxidation of the copper surface are still quite unknown. If we want to control the oxidation process, it is crucial to understand how the actual oxidation process begins and what are the next stages in the process. This works tries to seek answers for these questions using purely theoretical methods.

Previously, there has been discrepancy between the theoretical and experimental studies about the sticking coefficient on the clean Cu(100). According to the theoretical studies the oxygen molecule confronts no potential barrier as it approaches the surface. On the other hand, experiments have shown that such a barrier exists. That discrepancy is looked at using a different kind of approach, quantum mechanical molecular dynamics method. In this work it is suggested that the previously widely used method (PES) looses lots of information and therefore researchers can not rely on that method only. For the clean copper surface we found that when the molecule was given high initial kinetic energy towards the surface the previous calculations, which gave dissociative trajectories, are consistent with the ones performed here. On the other hand, when lower kinetic energies were used the molecule confronts a very intense steering effect and the trajectories lead to a molecular adsorbed states on the surface.

When the concentration of the oxygen exceeds 0.5 ML on the surface, the surface reconstructs. Similar methods have been used for the reconstructed surface. We found no dissociative trajectories for the reconstructed surface and, as for the clean surface, in molecular dynamics calculations a very intense steering effects were found.

TIIVISTELMÄ

Tekijä: Puisto, Antti

Nimi: **Oxygen adsorption on clean and O precovered Cu(100)**

Osasto: Sähkötekniikan osasto

Vuosi: 2004

Paikka: Lappeenranta

Diplomityö. Lappeenrannan teknillinen yliopisto. 49 sivua ja 35 kuvaa.

Tarkastaja: Professori Matti Alatalo

Hakusanat: Happi, hapettuminen, kupari, Cu, O, adsorptio

Kuparipinnan hapettumisen alkuvaiheet ovat vielä nykyisin tutkijoille epäselviä. Kuitenkin, jotta hapettumisprosessia voitaisiin säädellä, on sangen tärkeää ymmärtää mistä varsinainen hapettuminen lähtee liikkeelle ja mitkä ovat hapettumisen seuraavat vaiheet. Tähän kysymykseen haetaan vastauksia tässä työssä käyttäen puhtaasti teoreettisia menetelmiä pinnan käsittelyssä.

Aikaisempien teoreettisten ja kokeellisten tutkimusten välillä on pieni ristiriita liittyen hapen tarttumistodennäköisyyteen. Teoreettisten tutkimusten mukaan happi ei puhtaalle pinnalle tullessaan näe potentiaalivallia, mutta kokeelliset tutkimukset osoittavat sellaisen kuitenkin olevan. Tuohon ristiriitaan pureudutaan käyttäen aikaisemmista laskuista poikkeavaa kvanttimekaaniseen molekyylidynamiikkaan perustuvaa lähestymistapaa. Työssä havaitaan, että aikaisemmin yleisesti käytetty menetelmä hukkaa huomattavan määrän tietoa ja siten tutkijat eivät voi ainoastaan tyytyä tarkastelemaan kyseisellä menetelmällä saatuja tuloksia. Kuparipinnalle havaittiin, että korkeilla molekyylin kineettisen energian arvolla aikaisemmin suoritetut laskut hajottavista trajektoreista pitävät paikkansa, mutta matalilla kineettisen energian arvoilla molekyyli kohtaa erittäin voimakkaan "steering" vaikutuksen ja trajektorit joiden piti olla hajottavia johtavatkin molekulaariseen adsorptioon.

Kun hapen konsentraatio pinnalla on suurempi kuin 0.5 ML, pinta rekonstruoituu. Myös rekonstruktion jälkeistä pintaa on tutkittu samanlaisilla menetelmillä kuin puhdasta pintaa. Rekonstruoituneelle pinnalle ei löydetty hajottavia trajektoreita ja havaittiin, että hapelle annetun kineettisen energian matalilla arvoilla myös tässä tapauksessa on erittäin voimakas "steering" vaikutus.

PREFACE

This study is a part of the PINTA-project of Tekes and has been done for the Department of electrical engineering at Lappeenranta University of Technology.

I thank PhD Adam Foster, supervisor of this work, for his interest in my study and advisory. Thanks goes also to professor Matti Alatalo, the supervisor of this work, for advisory, support and proof-reading. I would also like to acknowledge my family for their support during my studies here at Lappeenranta University of Technology.

Contents

ABBREVIATIONS

ML	Monolayer
DFT	Density Functional Theory
LDA	Local Density Approximation
GGA	Generalized Gradient Approximation
VASP	Vienna Ab initio Simulation Package
SIESTA	Spanish Initiative for Electronic Structure with Thousands of Atoms
LCAO	Linear Combination of Atomic Orbitals
PES	Potential Energy Surface
MD	Molecular Dynamics
DOS	Density Of States
NEB	Nudged Elastic Band
TDDFT	Time Dependent Density Functional Theory

1 Introduction

In this study the adsorption of molecular oxygen on clean and O precovered, reconstructed $(2\sqrt{2} \times \sqrt{2})R45°$ copper [100] surface is examined using computational methods. The different phases of the process of copper oxidation are not well known and therefore more studies for the process were needed. Using computational *ab initio* methods the oxidation or any other process can be observed in more detail than by using the experimental methods only. This is because the experimental methods are bounded by the resolution of the measurement equipment and therefore cannot observe most processes at the atomic scale. By the computational methods one can also observe density of states and bonding which can be deduced from the experimental data but are not necessarily directly measurable. The reasons mentioned above have lead to the gain of popularity of the computational methods in addition to the experimental methods. The methods complement each other, for using both of these methods researchers can gain more accurate results more easily.

1.1 Objective

This study is a part of the research of the oxidation process of copper. This story begins with the handling of the clean copper surface and continues when there is already some oxygen on the surface and the surface is already reconstructed because of the oxygen. It is agreed [1], that clean copper surface is not reconstructed, the $c(2 \times 2)$ reconstruction appears at coverages lower than 0.34 ML (monolayer) and it does not appear in large well ordered areas, the $(2\sqrt{2} \times \sqrt{2})R45°)$ reconstruction of the surface occurs on oxygen coverages of over 0.34 ML. According to theoretical studies [2] the driving force for the latter reconstruction is the long range Coulomb interaction. This, and the fact that the Coulomb lattice energy is higher for the $c(2 \times 2)$, indicates that the $c(2 \times 2)$ reconstruction is not a stable reconstruction for copper and therefore it is justifiable to study only the $(2\sqrt{2} \times \sqrt{2})R45°)$ reconstruction. To continue the oxidation, more oxygen is needed. The intention of this study is to investigate how the molecular oxygen gets to the surface, whether the bond between the two oxygen atoms will break or the whole molecule will be adsorbed on the surface. The results of this study will hopefully give us more knowledge of the oxidation phenomenon.

1.2 Motivation

The classical oxidation theory for metals [3] suggests that the oxygen molecules do not adsorb to the surface, but the molecules or atoms above the surface create an electric field that pulls the metal atoms from the surface. This is, however, not what the modern experiments [4],[5] have shown so far. In these studies it is suggested that the metal oxidation would be the result of diffusion of the oxygen atoms in the metal surface. This and the fact that copper is gaining popularity to be used in microelectronics act as motivation to our calculations. Oxidation of copper causes dramatic changes in its conductivity properties. On the other hand it would be nice to be able to understand the process in detail, because then we might be able to control the process and in certain situations to speed up the process to form oxide layers and in others to slow down the process to prevent the oxidation. The understanding of this process would also be fundamental in understanding industrially very interesting phenomena such as bulk oxidation and catalysis.

2 Previous studies

Because the metal oxidation is so closely related to industrially important processes such as bulk oxidation, corrosion and catalysis, it has been studied earlier by many researchers. When looking at this problem more comprehensively one can see that understanding this phenomenon might work as a prototype, giving substantial understanding of the interaction between solids and gases.

2.1 Theoretical studies

In an earlier study *ab initio* methods have been utilized in for examining the adsorption of atomistic oxygen on a clean copper surface [6]. Those studies are closely related to this one. In that case the results were quite similar to the results gained from the experiments and other theoretical studies.

To gain the results the surface was first allowed to relax geometrically so that the atoms were at the positions which were energetically most favorable for the surface. As results relaxation depths for the clean copper surface were gained. Next, comparisons of the total energies and the adsorption energies of the different copper systems and oxygen in different geometric sites were made. The different adsorption sites are shown in figure 2.1

Figure 1: Schematic figure showing the symmetric adsorption sites on a clean Cu(100).

On clean Cu(100) surface there exist three symmetric sites where the oxygen might adsorp. The sites are on the top of a copper atom, between two copper atoms and between four copper atoms. The sites are called top, bridge and hollow, respectively. Also the surface with a vacancy was studied. By vacancy here is meant a site where there is one copper atom missing from the surface. In these studies it was determined that the
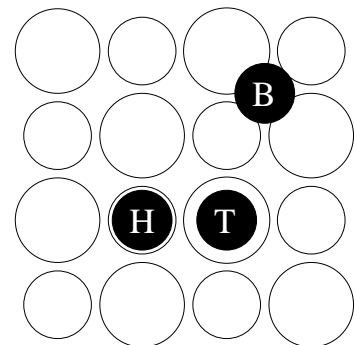
atomistic oxygen will most likely adsorb in the hollow site of the copper surface even if there exists a vacancy in the surface. This result was very surprising since one would expect that the most favorable site would be the vacancy.

Atomic and molecular oxygen on a clean Cu(111) surface has been studied using first principles methods by Xu and Mavrikakis [7]. They found that the atomic oxygen preferentially adsorbs to the three fold hollow sites favoring slightly the fcc site. Upon the adsorption the copper atoms in the surface show moderate relaxation. These results are consistent with the results calculated by Pitkänen [8]. For the molecular oxygen Xu and Mavrikakis found that O_2 binds to the surface in several energetically quasidegenerate states. They also found a single most favorable state in which the magnetic moment is quenched. The state has binding energy of -0.55 eV, so it is supposed to be quite stable. It is located above the bridge site molecular axis pointing to the top sites. Also other almost as favorable state was found. The other state has a magnetic moment of 1.0 μ_B and binding energy of -0.44 eV and is located above HCP site with molecular axis pointing towards the bridge sites..

The reconstructed surface has been studied by Stolbov and Rahman [9] with *ab initio* methods. They performed a careful geometric examination of the surface and several calculations concerning the reasons for the reconstruction. They came to the conclusion that the driving mechanism for the overlayer reconstruction is the long range Coulomb interaction which is in the case of copper stronger than the *p*O-*d*Cu covalent bonding for the c(2×2) reconstruction and therefore drives the formation of the overlayer. This is a slight drawback for the *ab initio* methods used today as they are not able to account for the long distance Coulombic force if very large supercells are not used. Using so large supercells is not possible because the capacity of the modern computers is not on that level yet.

2.2   Experimental studies

Copper oxidation can be experimentally studied by many different methods. The methods used include X-ray diffraction, low energy electron diffraction, surface extended X-ray

absorption and photoelectron diffraction. They have all proved to be very useful in surface measurements although time to time the experimental measurements give conflicting information.

There exist a number of experimental studies about the subject at hand [10, 11]. In reference [10] Robinson and Vlieg studied the structure of the $c(2\times2)$ and the $(2\sqrt{2}\times\sqrt{2})R45°$ reconstructions using X-ray diffraction. Both of the studies got similar results that the $(2\sqrt{2}\times\sqrt{2})R45°$ reconstruction is the stable reconstruction and that the $c(2\times2)$ reconstruction does not appear in large well ordered areas but only in nanometer sized islands and that it only appears on coverages lower than 0.34 ML.

Wöll *et al* [12] used in their work low-energy-electron-diffraction method. They confirmed that the only stable reconstruction for Cu[100] is the $(2\sqrt{2}\times\sqrt{2})R45°$ reconstruction. In their study they did not find any indication of the coexisting regions of the $c(2\times2)$.

3   Computational methods

3.1   Theoretical basis of the calculations

The methods used are based on the Density Functional Theory (DFT) which is originally stated in references [13, 14]. Using DFT one can in principle calculate, with just the knowledge of the atomic number, the cohesive characteristics of matter, energy band structures, magnetic properties and so on. The DFT can be applied for different particles although we here concentrate on electrons.

3.1.1   The principles of the Density Functional Theory

Suppose we have a many body system. There are N electrons in an external potential which is denoted by $V_{ext}(\mathbf{r})$ at locations $\mathbf{r}$. Let us restrict ourselves to consider the elec-

trons only and for simplicity forget the electron spin.

By the principles of quantum mechanics one can calculate the properties of the system using the Schrödinger equation

$$H\Psi = E\Psi, \tag{1}$$

where Ψ is the manybody wave function and the Hamiltonian H reads as follows

$$
\begin{aligned}
H &= \sum_i \left(-\frac{\hbar^2}{2m} \nabla_i^2 \right) + \sum_i V_{ext}(\mathbf{r}_i) + \frac{1}{2} \sum_{i \neq j}^N \frac{e^2}{|r_i - r_j|} \tag{2}\\
&= \hat{T} + \sum_i V_{ext}(\mathbf{r}_i) + \hat{V}, \tag{3}
\end{aligned}
$$

where $\hat{T}$ is the kinetic energy term, $\hat{V}$ is the potential caused by the electron-electron interaction. Thus, the electron density can be written as

$$n(\mathbf{r}) = N \int d\mathbf{r}_N |\Psi|^2. \tag{4}$$

When normalizing the wavefunction such that, using bracket notation, $\langle \Psi | \Psi \rangle = 1$, it follows that

$$\int d\mathbf{r}\, n(\mathbf{r}) = N. \tag{5}$$

The essential quantity of the density functional theory is the electron density. This is because one wants to avoid the calculation of the many dimensional wavefunction, since solving such a wavefunction is so painstaking and in most cases impractical. The theorem itself states that all the characteristics of a system can be calculated implicitly from the density of the particles.

The theory can be proven quite easily. Suppose that the ground-state of the system in question is non-degenerate. Then the external potential $V_{ext}(\mathbf{r})$ gives a unique ground-state wavefunction as a result of the Schrödinger equation. The electron density can be calculated from the wavefunction which means that the electron density can be calculated from the external potential. Thus, the electron density is a functional of the external potential. Therefore by knowing the density, one is able to calculate the external potential and the Hamiltonian of the system. When one knows the Hamiltonian of the system, he will be able to solve the wavefunction from the Schrödinger equation and therefore all the ground-state properties. When grouping all the functionals in an equation, it follows that

$$E[n(\mathbf{r})] = V_{ext}[n] + F_{HK} = \int n(\mathbf{r})V_{ext}(\mathbf{r})d\mathbf{r} + F_{HK}[n], \tag{6}$$

where V_{ext} is the external potential caused by the density n, F_{HK} is the Hohenberg-Kohn functional, which operates only on density and is universal such that the form of the functional does not depend on a particular system. The functional can be expressed in terms of Ψ, V_{eff}, and T with the notation

$$F_{HK}[n] = \langle \Psi | \hat{T} + \hat{V} | \Psi \rangle |_{n \to \Psi}. \tag{7}$$

The Hohenberg-Kohn second theorem suggests that for a trial density $\tilde{n}$ such that $\tilde{n} \neq n$ and $\int \tilde{n}(\mathbf{r}) = N$

$$E_0 \leq E[\tilde{n}]. \tag{8}$$

This is called the variational principle and it can be proven by substituting the trial density $\tilde{n}$ and the corresponding wave function $\tilde{\Psi}$ into 6

$$\langle \tilde{\Psi} | H | \tilde{\Psi} \rangle = \int \tilde{n}(\mathbf{r})V_{ext}(\mathbf{r})d\mathbf{r} + F_{HK}[\tilde{n}] = E[\tilde{n}] \geq E[n] = E_0. \tag{9}$$

3.1.2 The Kohn-Sham equations

When considering noninteracting particles the Hamiltonian can be written as

$$H_S = T + V_{ext} = \sum_i \left(\frac{\hbar^2}{2m} \nabla_i^2 + V_{ext}(\mathbf{r}_i) \right) \tag{10}$$

As one can see the variables in the Schrödinger equation for the system can be separated such that the resulting wave function would then be

$$\Psi_S(\mathbf{r}_1, \mathbf{r}_2, \mathbf{r}_3 \dots \mathbf{r}_N) = \psi_1(\mathbf{r}_1)\psi_2(\mathbf{r}_2)\psi_3(\mathbf{r}_3) \dots \psi_1(\mathbf{r}_N). \tag{11}$$

The one-particle wave functions ψ_i can be placed into the Schrödinger equation such that

$$\frac{\hbar^2}{2m} \nabla_i^2 \psi_i(\mathbf{r}) + V_{ext}(\mathbf{r}_i)\psi_i(\mathbf{r}) = \epsilon_i \psi_i(\mathbf{r}). \tag{12}$$

After that, if one considers the symmetry properties of the fermion wave functions, the exact result for the system would be the Slater determinant consisting of the ψ_i which satisfy the equation (12). The density of electrons can be written as

$$n(\mathbf{r}) = \sum_{i=1}^{N} |\psi_i(\mathbf{r})|^2, \tag{13}$$

where the sum is over the N lowest energy states.

To go further in the Kohn-Sham equations one must consider the notation

$$T_S[n] = \langle \Psi_S | T | \Psi_S \rangle \tag{14}$$

in which the $T_S[n]$ simply states the kinetic energy of a system without taking the particle interactions into account. The functional $T_S[n]$ can be used to define the total energy of a system without interactions using the following equation

$$E[n] = T_S[n] + \int V_{ext}(\mathbf{r})n(\mathbf{r})d\mathbf{r}, \tag{15}$$

which can be stated using the Euler equation

$$\frac{\delta T_S[n]}{\delta n(\mathbf{r})} + V_{ext}(\mathbf{r}) = \mu, \tag{16}$$

where μ is represents the electro chemical potential of the matter. By solving the last equation one gets the exact ground state density which, as shown in the previous section, then assigns all the ground state properties.

When considering everything noted above in a system with interactions the functionals in the Schrödinger equation can be stated as follows.

$$
\begin{aligned}
H &= T + U_{el} + V_{ext} \\
E &= E[n] = T_S[n] + V[n],
\end{aligned}
$$

where $V[n]$ is an unknown functional for the time being and the functional $T_S[n]$ is the kinetic energy of the noninteracting system. Using the notation

$$V_{eff}(\mathbf{r}) = \frac{\delta V[n]}{\delta n(\mathbf{r})}, \tag{17}$$

the above Euler equation can be written in the following form

12

$$\frac{\delta T_S[n]}{\delta n(\mathbf{r})} + V_{eff}(\mathbf{r}) = \mu. \tag{18}$$

As one can see, equations 18 and 16 can be compared and the result for equation 18 can be stated as

$$n(\mathbf{r}) = \sum_{i=1}^{N} |\psi_i(\mathbf{r})|^2, \tag{19}$$

where obviously the $\psi_i(\mathbf{r})$ must satisfy the differential equation

$$-\frac{\hbar^2}{2m}\nabla^2\psi_i(\mathbf{r}) + V_{eff}(\mathbf{r})\psi_i(\mathbf{r}) = \epsilon_i\psi_i(\mathbf{r}). \tag{20}$$

The equations 17, 19, and 20 are called the Kohn-Sham equations. From these equations it is possible, in principle, to solve the interacting many body system ground state density in exact form. The missing link in these equations is the effective potential V_{eff}. The V_{eff} can be stated using the exchange and correlation energy E_{xc}

$$V_{eff}(\mathbf{r}) = e\phi(\mathbf{r}) + \frac{\delta E_{xc}[n]}{\delta n(\mathbf{r})}. \tag{21}$$

where E_{xc} can be denoted

$$E_{xc}[n] = E[n] - T_S[n] - V_{ext}[n] - H[n]. \tag{22}$$

Unfortunately only the $V_{ext}[n]$ of those functionals is known. For solving the exchange and correlation energy there are a number of ways to go. In the Local Density Approximation (LDA) the E_{xc} is calculated using the electron density of the homogenous electron gas

$$E_{xc}[n] \approx \int d\mathbf{r} n(\mathbf{r})\epsilon_{xc}(n(\mathbf{r})). \tag{23}$$

Actually this approximation is surprisingly good although it looks simple. In the case of semiconductors and insulators the results are not as good as in the case of metals because LDA tends to underestimate the energy gaps. This is due to the fact that the exchange correlation potential is supposed to be different for the valence and the conduction bands and so it would have to be discontinuous and a function of electron number. This under-estimation of the band gap leads to problems when trying to solve for example the states induced by a defect in a semiconductor or insulator. In this case when one is studying metals this problem is negligible because the conduction and the valence bands overlap and there is no gap between them. Here we used the Generalized Gradient Approximation (GGA). The GGA is like the LDA, but it also uses the gradient of the electron density. There exists some sort of consensus within scientists that the GGA is better than LDA for surface calculations, because the local densities change so rapidly in surfaces.

3.2   Basis sets and pseudopotentials

In numerical calculations the wave functions for the electrons have to be expressed using some sort of basis functions. These basis functions may be for example plane waves or atomic orbitals. When solving the systems one notices that the wave functions consist of Fourier series (because of the basis functions) which goes on to infinity. It follows that one has to cut the series after some certain finite number of elements.

When looking at the core electrons in the deep Coulomb potential, their wave functions are more rapidly changing and therefore denser sampling is needed to describe their wave functions. This causes that the computation takes longer for the core electrons. The core electrons do not determine most of the chemical properties of the material but the valence electrons do so this use of computational time is generally unnecessary. One way of avoiding this unnecessary computational cost is to use so called pseudopotential method. The method is based on the idea of not including the core electrons and their rapidly changing wave functions in the calculations, but replacing the effect of core electrons with a smoother function which can be solved by using less basis functions. As noted before the core electrons do not take much part for the chemical reactions and therefore this procedure is acceptable.

Of course, the pseudopotentials need careful testing before using them to solve any system. The testing can be made by calculating a well known system using the pseudopotential of which one wants to test. The results should be preferably compared to an all electron calculation of the same system and not to the experimental results. This is because the calculations make also other approximations and thus are not quantitatively comparable with the experimental results. The measures that can be used to compare the pseudopotential are for example the lattice constant or the bulk modulus. The latter is not too good a test measure, though, because it is a second derivative of a numerical quantity and therefore cannot be obtained as accurately as e.g. the lattice constant.

4   Testing the simulation parameters

The used programs need to take some simulation parameters as input. These parameters are determined with a few less time consuming calculations, because all of these parameters are transferable from one system, consisting of the same atom type, to another. The results of testing the simulation parameters are shown in this section.

4.1   Programs

The programs used in the simulations are VASP (Vienna Ab Initio Simulation Package) [15],[16] for some of the PES-plots (Potential Energy Surface, see section 5) and for comparison and SIESTA (Spanish Initiative for Electronic Structure with Thousands of Atoms) [17],[18] for most of the PES-plots. The VASP method uses ultrasoft pseudopotentials and plane waves to calculate the groundstate properties of a system while the SIESTA method uses the linear combination of atomic orbitals (LCAO) and norm conserving pseudopotentials [19],[20],[21].

The SIESTA code is a linear scaling code (where here we have used linear scaling only in the construction of the Hamiltonian to preserve accuracy), which allows one to calculate very large systems with less cpu time and that is why it was chosen for the PES

calculations. For the VASP code the scaling is about N^3 where N is the number of atoms and therefore it is not very suitable for calculating very large systems but the accuracy for the results of the plane wave calculations is easier to determine than with the atomic orbitals: Using more plane waves makes the calculations more accurate. On the other hand increasing the number of atomic orbitals does not necessarily lead to more accurate results.

Due to different basis and pseudopotentials the total energies cannot be compared between VASP and SIESTA. Though, the lattice constant and other structural properties should be comparable. The PES-plots are supposed to be comparable when not looking at the absolute energy scales.

For plotting the charge density figures programs called OpenDX and Gopenmol [22], [23] were used. In the charge density plots different scales were used because the two programs are not compatible with each other. OpenDX had to be used for the charge density figures calculated with VASP. This was because we found no way to convert the output of VASP into any format that would have been compatible with Gopenmol.

4.2   Pseudopotentials for VASP

With the VASP package there is delivered a comprehensive set of pseudopotentials which are tested to work. One can not rely completely on the tests made by others because the risk that the pseudopotential is no good is up to the user. To test the pseudopotentials two calculations were needed. First to test the pseudopotential for copper a bulk calculation was made with different lattice constants. The lattice constants and total energies are shown in table 1 and in figure 2. The experimental value for the lattice constant of copper is 3.615 Å [24]. As seen in the table the calculations give a lattice constant, which is very close to the experimental value. Secondly to test the pseudopotential for the oxygen a calculation where the oxygen molecule was let to relax to its bonding distance was done. The result was more than acceptable 1.242 Å whereas the experimental value is 1.207 Å [24].

a [Å]	E_{tot} [eV]
3.50	-3.673
3.52	-3.697
3.54	-3.717
3.56	-3.733
3.58	-3.745
3.60	-3.754
3.62	-3.759
3.64	-3.762
3.66	-3.761
3.68	-3.757
3.70	-3.751
3.72	-3.742
3.74	-3.733
3.76	-3.720
3.78	-3.705
3.80	-3.689

Table 1: Total energy for different lattice constants in copper bulk.
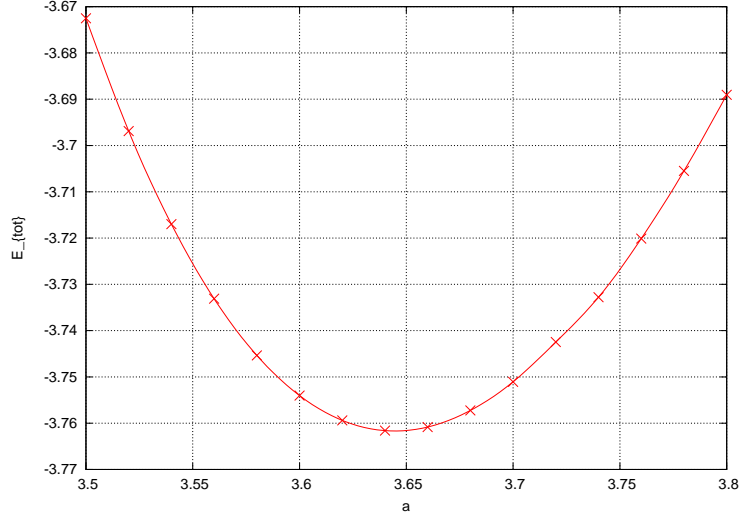
Figure 2: Total energy vs the lattice constant for copper bulk calculated with VASP. The minimum of the plot gives the optimum lattice constant.

4.3 K-points

K-points represent the sampling of the first Brillouin zone in the k-space and therefore it has a great influence on the results gained from the calculations. This makes it obvious that the sampling set should be very carefully chosen. The smallest slab was relaxed with different k-point meshes to find out which k-point set to use during the next simulations. This is an important step because the accuracy of the simulations depends considerably on the used k-point mesh. The mesh can be chosen by a number of methods, but one of the most popular choices is the Monkhorst-Pack [25] mesh.

In the Monkhorst-Pack mesh the k-points lay homogeneously on the Brillouin zone. The Monkhorst-Pack mesh can be expressed using the equation

$$k = x_1 b_1 + x_2 b_2 + x_3 b_3, \tag{24}$$

17

	5×3×1	6×4×2	7×5×1	7×6×1	8×7×2	9×8×2
E_{tot}[eV]	-190.4460	-190.2968	-190.4315	-190.3993	-190.3924	-190.3992
Δ_{12}[%]	6.6868	6.8736	6.7033	6.6978	6.7527	6.7473
Δ_{23}[%]	2.0385	3.0110	2.2253	3.0769	2.3681	2.3681
Δ_{34}[%]	1.8736	2.3736	1.8681	2.4560	1.8901	1.9011
Δ_{45}[%]	1.1374	2.1044	1.3242	2.0495	1.4451	1.4505
Δ_{56}[%]	-2.0220	-1.1538	-1.9286	-0.9835	-1.7967	-1.8022

Table 2: Total energies and relaxations between different layers calculated with different k-point meshes for the reconstructed surface. The slab used in the calculation had eight surface atoms in the non-reconstructed layers and six copper atoms and four oxygen atoms in the reconstructed layer.

where b_1, b_2 and b_3 are the reciprocal lattice vectors and

$$x_i = \frac{l}{n_i}, \ l = 1 \ldots n_i.$$

It is well known that the Monkhorst-Pack scheme does not cause the total energy to converge very well for the hexagonal lattices, but since copper crystallizes as an fcc lattice it was OK to use the Monkhorst-Pack scheme for the K-points.

The results of the k-point calculations are shown in table 2. Judging by the table the Monkhorst-Pack mesh of 7×5×1 was chosen to be sufficient for these calculations and therefore was used in further simulations for the smallest slab. It is suggested that the amount of k-points can be roughly estimated using the equation for the calculations to be consistent with each other

$$N_x \times N_y \times N_z \times N_{\text{atom}} \approx \text{C} \tag{25}$$

where N_x is the amount of k-points in the x direction, N_y in the y direction, N_z in the z direction, N_{atom} is the number of atoms in the system and C is constant [26].

As one can see in the table 2, larger amount of k-points is not always better when choosing

Supercell	k-point mesh	atoms	irreducible k-points
4×4×6	7×5×1	50	12
4×6×6	7×3×1	75	12

Table 3: Used k-point meshes for the simulated supercells. The Supercell-column shows the size and shape of the supercell in the form {*atoms in x-direction*}×{*atoms in y-direction*}×{*atoms in z-direction*}. The k-point mesh-column shows the k-point grid in the same order as the Supercell-column. The atoms-column indicates the number of atoms in the supercell and the irreducible k-points-column shows the amount of k-points in the first Brillouin zone that can not be reduced by the symmetry.

the mesh because the results depend intensively on how the k-points reside in the Brillouin zone. In principle, it is always a good idea to use lots of K-points when calculating metals because of their special properties. Too small amount of K-points may cause the calculation to show a band gap in metal which is simply wrong. On the other hand, choosing more k-points makes the calculation heavier with respect to the computer time. The suitable meshes for the other used supercells were calculated by the equation 25. The used meshes are shown in the table 3

Other issues concerning the K-points are the size and the symmetry of the slab. When using larger supercells smaller amounts of K-points are needed. This fact is also applied here. On the other hand it is wise to use more K-points in the dimensions were the symmetry is more broken. As a result of these arguments and when looking at the system considered here more K-points were needed in the x-dimension than y-dimension since the supercell is wider in the y-dimension and the symmetry is more broken in the x-dimension because of the missing row. This can also be seen in table 3.

4.4 Cut-off energy

When using VASP, or any other planewave method, the terms of the series used in describing the wave functions can be expressed in terms of their energy. When the series is cut out after a certain term the energy of the term is called the cut-off energy. The cut-off energy should be large enough such that the total energy is already converged. In this

work the cut-off energy of 380 eV was used. It was determined in the previous calculations. If only copper would be calculated then 330 eV would have been sufficient enough, but the pseudopotential for oxygen converges so slowly that higher cut-off was needed. The test for the pseudopotential of copper is documented in table 4 and in figure 3

E_{cut} [eV]	E_{tot} [eV]
170	-3.174746
210	-3.661694
250	-3.705438
290	-3.705184
330	-3.700127
370	-3.698695
410	-3.699048
450	-3.699168
490	-3.698925
530	-3.698628
570	-3.698457

Table 4: Test data for the cut-off energy.
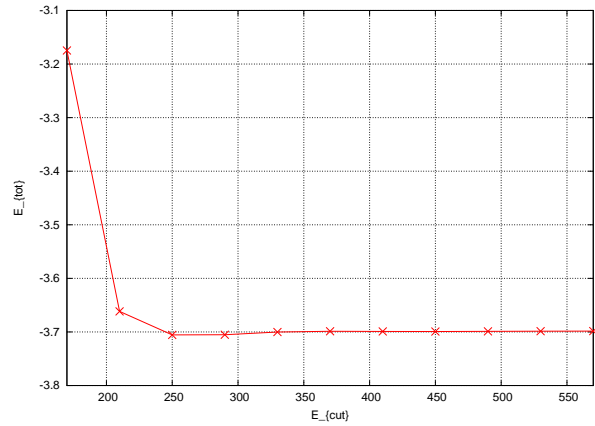
Figure 3: The total energy for bulk copper versus the cut-off energy calculated with VASP.

4.5 From VASP to SIESTA

Because making the calculations with VASP was so time consuming, a large part of the simulations were made using SIESTA instead. Before beginning the actual simulations with SIESTA a careful set of tests was made to ensure that the pseudopotentials and the basis sets were good. In the next few subsections these tests and their results are introduced.

4.5.1 Testing the pseudopotential for copper using SIESTA

The pseudopotential for copper was tested with a simple bulk calculation. In this test the total energy for the bulk was calculated with a few different lattice constants. The results for this test are shown in table 5. The values from the table are plotted in figure 4.

a_{lat} [Å]	E_{tot} [eV]
3.63	-6207.591
3.66	-6207.729
3.69	-6207.832
3.72	-6207.904
3.75	-6207.947
3.76	-6207.955
3.77	-6207.961
3.78	-6207.962
3.785	-6207.963
3.79	-6207.938
3.80	-6207.934
3.81	-6207.926
3.84	-6207.892
3.87	-6207.840
3.90	-6207.773
3.93	-6207.692

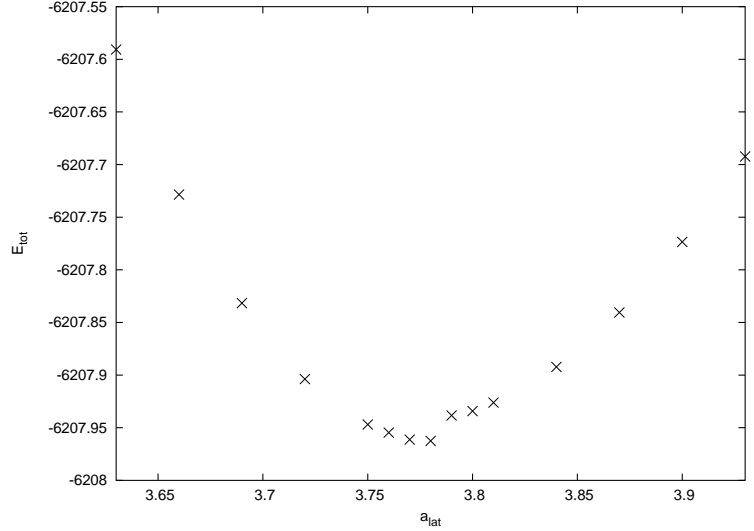Table 5: Total energy for different lattice constants in bulk copper.

Figure 4: Total energy vs the lattice constant for bulk copper calculated with SIESTA. The minimum of the plot gives the optimal lattice constant.

The minimum for the total energy indicates the lattice constant that is right for this pseudopotential and basis set. In this case it is around 3.785 Å which is somewhat larger than the 3.64 Å which was calculated using VASP and Vanderbilt type ultrasoft pseudopotential.

4.5.2 Mesh cut-off

When using SIESTA the mesh cutoff parameter describes the accuracy of the calculation when compared against the plane wave calculations. It is not the same value but it describes the same issue when scaled with some factor. For the mesh cut-off a few values were tested with copper in bulk. Those values are documented in table 6 and figure 5. For further calculations the mesh cut-off of $150 \ \mathrm{Ry} = 2040$ eV was seen suitable.

E_{cut} [eV]	E_{tot} [eV]
49.780	-6222.473
63.003	-6210.731
112.006	-6208.527
175.009	-6208.007
199.122	-6208.001
252.014	-6207.935
311.128	-6207.915
448.024	-6207.899
486.137	-6207.905
567.031	-6207.902
700.038	-6207.899
796.487	-6207.899

Table 6: Test data for the mesh cut-off.
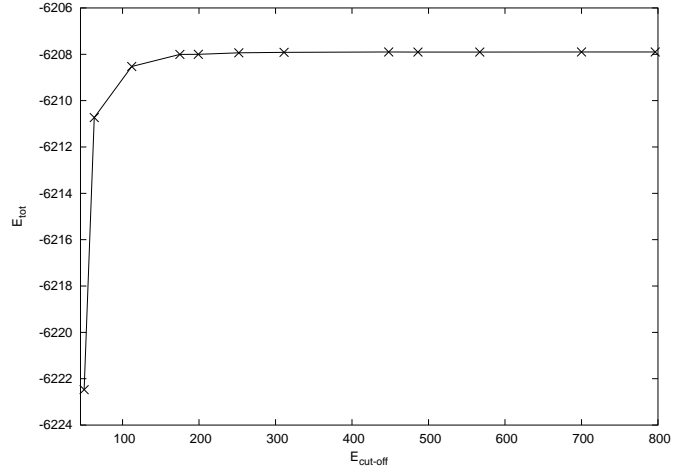
Figure 5: The total energy for copper bulk calculated against the mesh cut-off with SIESTA.

4.5.3 Testing the basis set

SIESTA uses atomic orbitals and therefore one has to define the basis set for the orbitals to be able to do any calculations. For Cu the basis set was optimized by comparing the calculated lattice parameter to the experimental one. As seen in figure 4 the lattice parameter is not as close to the experimental parameter as it is when using VASP, but the value differs only about 5 percent from the experimental value of 3.615 Å and therefore it is acceptable. This was acchieved using one ζ in the polarization orbital.

The basis for oxygen was tested by calculating a system, which contained an oxygen molecule and comparing the bonding distance to the experimental value. The calculation was repeated using different amount of ζ in the basis. The results for these calculations are shown in table 7. Judging by the table two ζ for both quantum numbers l was seen sufficient. On the other hand, the basis set for oxygen was tested by calculating the structure of copperoxide Cu_4O_3, to be more precise. While comparing the structural properties of the system, it was seen that only one ζ for both quantum numbers would be enough for the oxygen in the oxide.

l	0	1	0	1	0	1	0	1	0	1
polarization	n	n	P	P	P	P	P	P	P	P
ζ	0	0	1	1	1	2	2	2	3	3
r_{bond}	1.289		1.241		1.238		1.237		1.236	

Table 7: Tested ζ for the molecular oxygen.

l	0	1	0	1	1	0	0	1	0	1
polarization	n	n	P	P	P	P	P	P	P	P
ζ	0	0	0	1	1	1	1	2	2	2

Table 8: Tested amount of ζ in the polarization orbitals for oxygen. n indicates no polarization orbitals. In the table P means that polarization orbitals were used in the calculation.

4.5.4 Slab calculation

As a prototype case a surface calculation was performed for testing purposes. The results were quite similar when calculated with SIESTA or VASP. Of course the larger lattice constant made the dimensions of the surface a bit larger but the relaxation was about the same size as with VASP calculations. The resulting data is documented in table 9. When calculating the overall relaxation one can notice that the relaxation is in the same direction for both of these calculations. Also it is worth pointing out that all of the calculated quantities are of the same order, however SIESTA tends to underestimate the relaxations when compared to VASP. This might be due to the differences in the used pseudopotentials. When comparing both of these results to the experimental ones [28] [29], the results calculated with SIESTA seem to be more consistent with the experimental results. Judging by these results it can be fairly said that there seems to be nothing suspicious going on and therefore we are good to go ahead with these calculations.

4.5.5 The reconstructed surface

As another prototype case the a calculation for the reconstructed surface using SIESTA was performed. The results are collected in table 9. The results clearly indicate that the calculation performed using SIESTA is consistent with the plane wave calculation

Δ_{12}	Δ_{23}	Δ_{34}	Δ_{45}	Δ_{56}	Total
LEED					
-1.2	0.9	-	-	-	
VASP					
-2.51	1.68	1.68	1.49	-2.86	-0.52
SIESTA					
-0.95	0.43	0.51	0.47	-0.73	-0.28

Table 9: Relaxations between layers in slab calculation of Cu(100) surface, 8 surface atoms and six layers. The numbers are percents of the calculated lattice constant.

performed using VASP. The lattice constant for the case of calculation performed with SIESTA is somewhat larger. This was the case with the clean surface also and thus there is nothing special about it. The relaxations for both calculations are consistent with each other and with the experiments. Based on the arguments shown above it was safe to proceed the calculations using SIESTA instead of VASP.

5   Results

In this section the results of the simulations are shown. First, there are some results concerning the clean copper surface and the results for the molecular dynamics simulations for the oxygen molecule on the clean copper surface. Next, the Potential Energy Surface (PES) plots for the reconstructed surface are considered followed by the results of the molecular dynamics simulations for the reconstructed surface. Many Density Of States (DOS) plots are presented in order to explain the bonding in different situations, together with a few cuts of the electronic charge density to explain the bonding between the atoms at interest.

5.1   The Potential Energy Surface

The PES plot is a way of describing what kind of potential the molecule confronts when approaching the surface. Usually 3-dimensional cuts of the surface are presented as contour plots but the true surface itself is 6-dimensional. To create such a plot one needs to move the oxygen molecule towards the surface while varying the distance between the atoms that form the molecule. Because the PES calculations are static, which means that the atoms are not allowed to move, it is not yet clear how much we are missing, when using only PES calculations. For example the atoms in the surface might move from their initial positions to some other position and thus prevent the breaking of the oxygen molecule. Also the potential energy surface shows the minimum of the molecule, when the molecule has no kinetic energy. In reality the molecule will have kinetic energy, because the molecule is at some finite temperature. This is one reason why it is very interesting to do both MD and PES for the same situation.
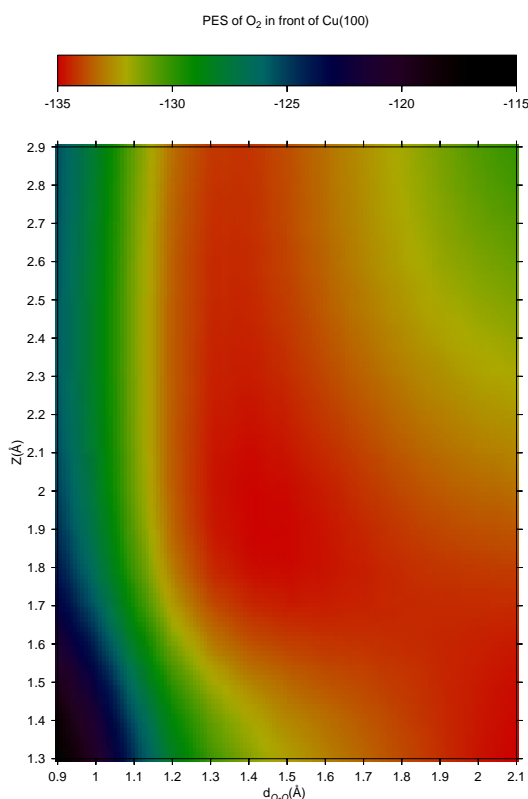
Figure 6: PES calculated by Alatalo *et al*.

Lets look at the physics behind the pretty PES figure using, as an example, PES calculated by Alatalo *et al.* in [27] for oxygen molecule on a clean Cu(100) surface. In figure 6 it can be seen that as the molecule is brought closer to the surface (vertical axis) the energy minimum moves to higher bond lenght values (horizontal axis). This indicates that as the molecule approaches the surface the bond lenght increases. In the minimum energy path the total energy seems to stay generally constant. This means that the molecule does not have to overcome any barrier inorder to get to the surface and break.

5.2   Molecular Dynamics

In molecular dynamics calculation all the ion cores are allowed to move by the forces acting on them. In molecular dynamics calculation the forces are usually calculated by the Newton equation which states

$$F = m_i a_i, \tag{26}$$

where F is the force, a_i are the accelerations of the ions, and m_i are the masses of the ions. For the ions such initial velocities are given, that conforms to the kinetic energy of the ions in certain temperature. During the calculation cycles the forces can be calculated by the change in the total energy when moving the ion from one place to other. This can be stated as

$$\frac{dE}{dr_i} = F_i, \tag{27}$$

where dE is the change in the total energy, dr_i is the change in the ion position, and F_i is the force acting on ion. One nice feature about MD calculations is that one can assign some initial velocity for the ions. This makes it possible to anneal the system to simulate actions in some finite temperature. Also, it is possible to steer, for example, the molecule towards the surface and thus simulate the collisions.

5.3 Results for the clean surface

5.3.1 Atomic oxygen on the clean surface

The calculations for the atomic oxygen on the clean Cu(100) surface were performed using VASP. The purpose of these calculations was to find out which one of the sites on the surface was most favorable for the oxygen. The studied sites were the four fold hollow site, the vacancy in the surface, and the bridge and the top sites on the surface. The calculated adsorption energies for the different sites are presented in table 10. Judging by table 10, the most favorable site for the oxygen on the surface is the four fold hollow site even if the surface contains a vacancy. From the top and the bridge sites the oxygen

Layer	E_{tot}	E_{ads}
1	-172.55771	-1.40613
2	-173.70427	-1.21239
hollow*	-117.57977	-2.42321
bridge*	-116.87893	-1.72238
top*	-115.72340	-0.56684
hollow + vacancy*	-113.40051	-2.44183
bridge + vacancy*	-112.78734	-1.82867
top + vacancy*	-111.67930	-0.72062

Table 10: Adsorption energies and total energies for atomic oxygen on the Cu(100) surface. In the table the Layer-column shows the location of the oxygen atom. Slab with 8 surface atoms was used in all of these calculations.
* Only four layers were used in these calculations and therefore the total energies are not comparable.

atom will fall to the sites that are lower in energy. When the oxygen is at the top site, there exists a barrier between the vacancy and the top site. This prevents the oxygen from moving from the top site to the vacancy. The same situation is encountered when the oxygen is at the bridge site. According to these calculations the top and bridge sites are local energy minima at least when there exists a vacancy in the surface. Of course, this should be confirmed by an MD calculation to be really sure. However, the barrier might be so small that the kinetic energy even in room temperature in the MD calculation might be able to kick the oxygen from the top or bridge site to the sites lower in energy. The results in table 10 clearly indicate that the most favorable site for oxygen on Cu(100) surface is the hollow site. When a vacancy is added to the surface the adsorption energy

for the oxygen in the hollow site will rise and the hollow site still remains as the most favorable site.
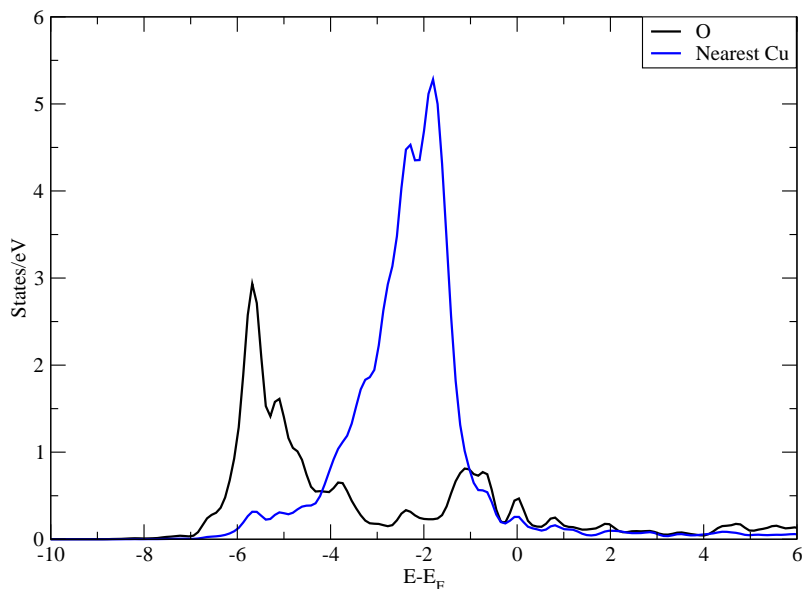
Figure 7: Density of states for the case where the oxygen is in the hollow site. Presented are the p-DOS of the oxygen and the d-DOS of the nearest copper.

The DOS for the case when the oxygen is in the hollow site is illustrated in figure 7. In the figure some bonding of oxygen to the first layer of copper atoms is observed. This can be said because in the figure some hybridization between the oxygen p density and the copper d density can be observed in the figure. For comparison, also the density of states for the top and bridge sites are shown in figure 8. In the DOS figure for the hollow site there is more occupation in the lower bonding state, and the bonding state seems to be lower in the energy. This makes the hollow site energetically more favorable. Also, the hollow site is more symmetric and therefore the oxygen has some bonding to all four neighbouring copper atoms.
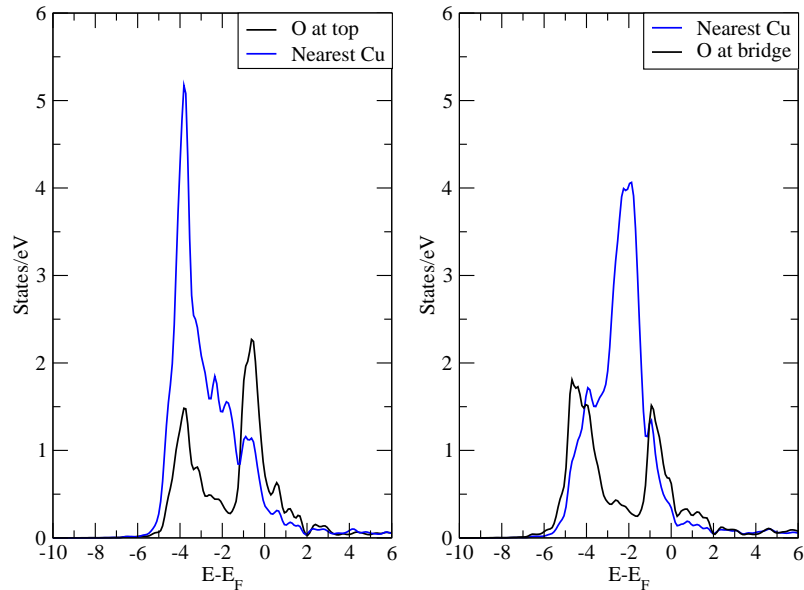
Figure 8: Density of states for the cases where the oxygen atom is at the top and bridge sites.

5.3.2 Oxygen molecule on top of the clean Cu(100) surface

The situations calculated using molecular dynamics are shown in figure 9. Based on the calculations done by Alatalo *et al.* [27] there exists a trajectory that splits the oxygen molecule that is adsorbing to the surface right above the top site. An MD simulation was performed to confirm that this trajectory exists and to see if there exists some sort of steering effect as the molecule approaches the surface. In the simulations temperature of 300 K for the surface was used (Nose thermostat) the bottom layer of the surface was fixed and kinetic energy of 1.8 eV and 50 meV, which correspond to 1500 K and 300 K, respectively, for the oxygen molecule was given. In both of these simulations the molecule is located horizonatally above the surface such that the middle of the molecule is straight above the top site and the center axis of the molecule is pointing towards the hollow sites. With the higher kinetic energy, the oxygen molecule will indeed break and the oxygen atoms will adsorb in the four fold hollow sites in both sides of the top site after 233 fs of simulation. No steering effect of any kind was seen in the simulations using the higher initial kinetic energy for the oxygen. When the lower energy was used, the oxygen molecule confronted a barrier above the top site, and faced some sort of steering effect.
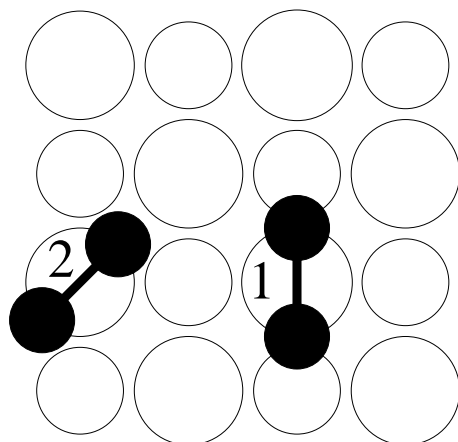
Figure 9: Schematic picture of the situations where molecular dynamics were applied.

The molecule finally moved after from the top site straight above the hollow site and did not break but molecularly adsorbed to the surface after 1038 fs of simulation. This is a clear indication, that when only the PES figures are calculated something interesting will most likely be missed. This is probably because of the static nature of the PES calculations or the too coarse grid used during the PES calculation. Also another MD calculation was performed using the position of case 2 as the initial position for the molecule. In that case also the molecule ended up in a similar molecularly adsorbed state when lower (50 meV) initial kinetic energy for the molecule was used. The adsorption energy for this molecularly adsorbed state found in these MD calculations for the clean surface was -1.3119 eV which indicates that this state is quite stable and therefore it most likely should be seen in the experiments, if the surface temperature is low enough and the oxygen molecules do not interact with each other during the tests.

5.4   Molecular oxygen on top of the reconstructed surface

The situations that we considered are shown in figure 10. To study these cases, we used Potential Energy Surface calculations and molecular dynamics calculations. Both of these calculations are very slow to perform and therefore we had to consider carefully which situations are more interesting than others.
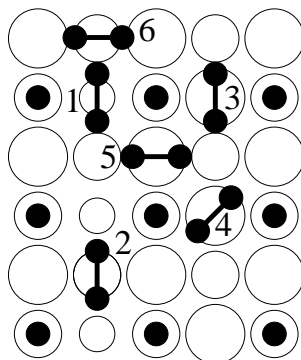
Figure 10: Schematic illustration of the situations considered within this study.

5.4.1 PES for O_2 on the reconstructed surface

PES plots were calculated for molecular oxygen adsorbing to the surface in orientations that are presented in figure 10, to get a picture of where the oxygen might adsorb in molecular form and where the bonding between the oxygen atoms might break. When looking the problem there is a possibility that the oxygen might approach the surface in infinite amount of different positions and therefore it is not possible to calculate all the possible combinations of the angles and the sites. Indeed, when carefully chosen only some of the combinations are needed to get a good picture of the situations.

5.4.2 Molecular oxygen in the missing row

In the missing row there are two sites that differ a great deal from each other by there symmetry. These sites are shown in figures 11 and 13 from the top view and in figures 12 and 14. Hereafter this the two situations will be referred to as case 1 and 2. As mentioned above also in the missing row there are infinitely many different sites, but their properties do not differ much and as so it is not reasonable to draw PES-plots of all of them. The PES plots for the situations explained above are shown in figures 15 and 16.

In both of these cases there exists a potential energy minimum at about the same height which is approximately 2.5 Å above the surface. This means that there exists some sort
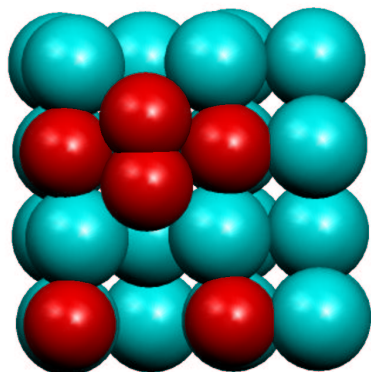
Figure 11: The oxygen on the surface in its energy minimum from the top view.
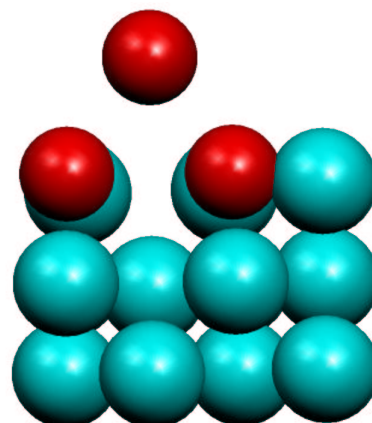
Figure 12: Same as figure 11 but side view.
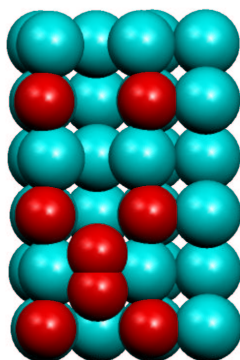
Figure 13: The oxygen molecule on top of the missing row in its energy minimum in case 2.
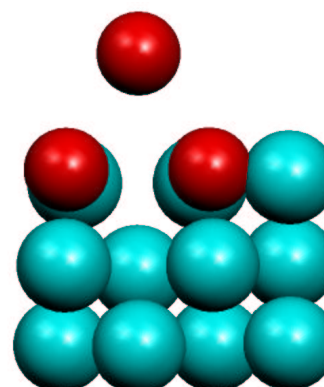
Figure 14: Same as figure 13 but side view.

of energy barrier between the molecule and the surface which the molecule needs to overcome in order to get to the surface. Also by looking at the plots one can notice that the bonding between the oxygen atoms is not going to break without external energy. Looking at the O_2 molecule point of view the minimum is at the natural bonding distance of the oxygen atoms in a molecule so by studying only the PES plots one might think that the molecule and the surface do not effect each other.

At this point it might be wise to consider the density of states in the potential energy
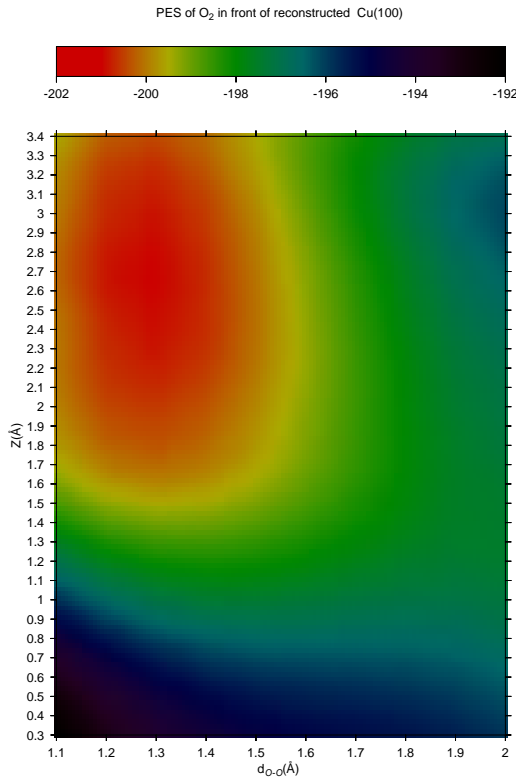
Figure 15: Potential energy surface for O$_2$ in case 1.
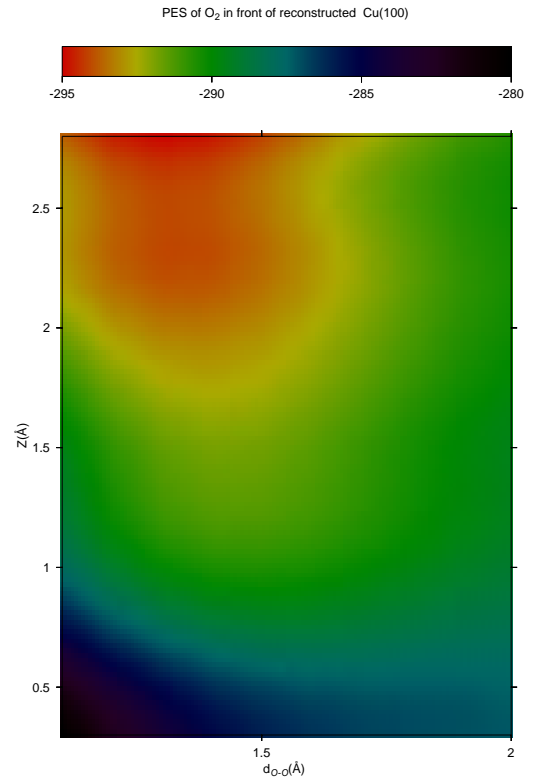
Figure 16: Potential energy surface for O$_2$ in case 2.

minimum for the oxygen atom and the copper atom which is nearest to it. In figures 17 and 18 the DOS-plots for the systems are shown. After carefully examining the DOS plot for the case 1, it is clear that the molecule and the surface effect each other. First of all, the spin up and spin down densities are symmetric for Cu. This is typical for a noble metal. The spin up and down densities for the oxygen are moved with respect to each other. This indicates some magnetic behavior and is also typical for an oxygen molecule. There exist lots of states in the bonding state of the insurface oxygen which is obviously tightly bonded to the surface. For the molecular oxygen, however, this is not the case. The p-DOS for the molecular oxygen looks remarkably similar to the p-DOS of a free oxygen molecule. Only the lowest spikes, that are typical for the molecule, are moved downwards, but the main picture in both of these cases is that the DOS of the molecule stays similar to that of the free molecule. In situation 2, however, the intensities of the spikes are affected by the surface atoms and therefore one can not say that the surface and the molecule do not interact with each other. Altough, in both situations the DOS seems
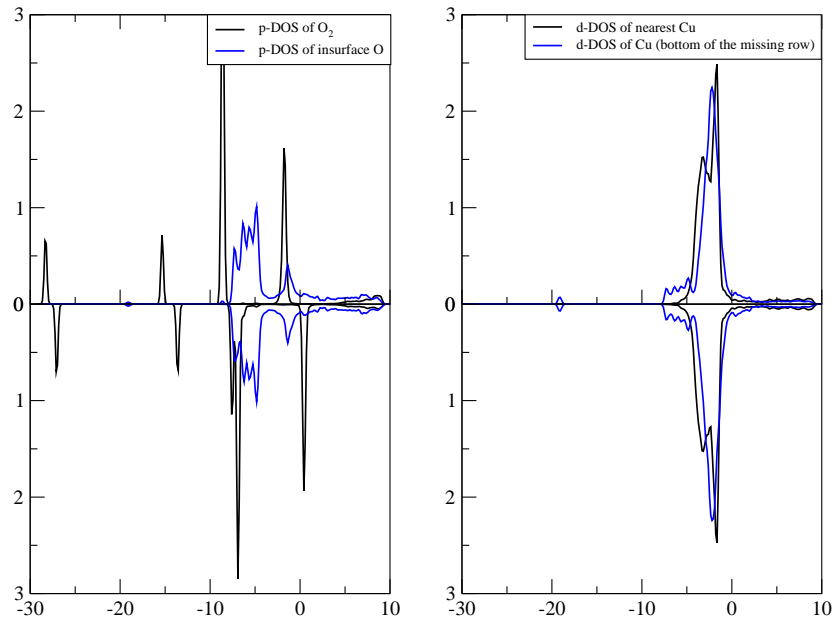
Figure 17: Density of states for the case 1. The upper part of the figure corresponds to the spin up case and the lower part presents the spin down.
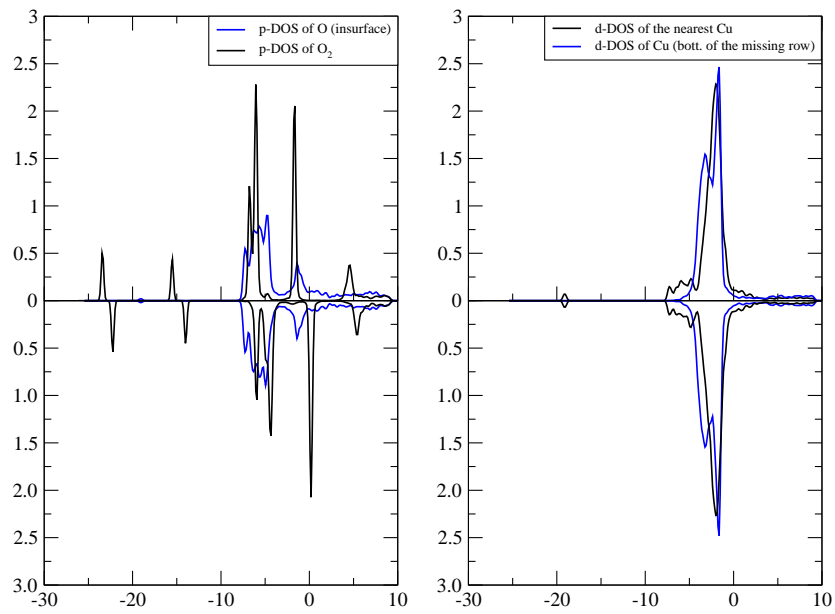

Figure 18: Density of states for the case 2. The upper part of the figure corresponds to the spin up and the lower part presents the spin down.

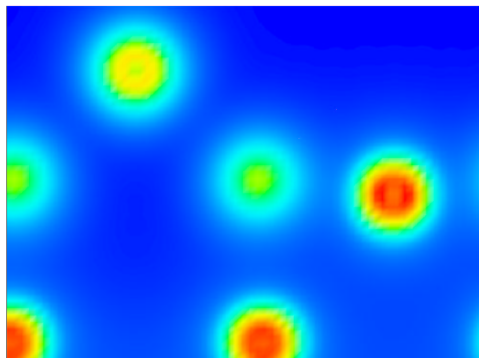to indicate that the oxygen remains in molecular form.

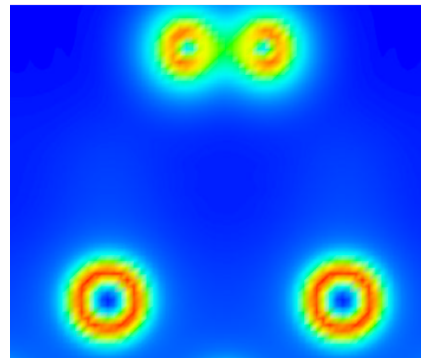Figure 19: Charge density of the oxygen molecule in the energy minimum above the surface in case 1. The upmost atom is the oxygen.

Figure 20: Same figure as figure 19, but orthogonal view. This is shown to see the bonding between the two oxygen atoms.
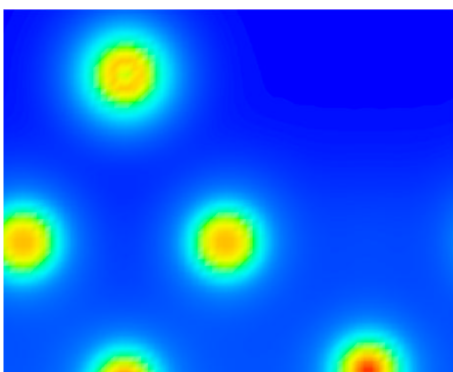
Figure 21: Charge density of the oxygen molecule in the energy minimum above the surface in case 2.
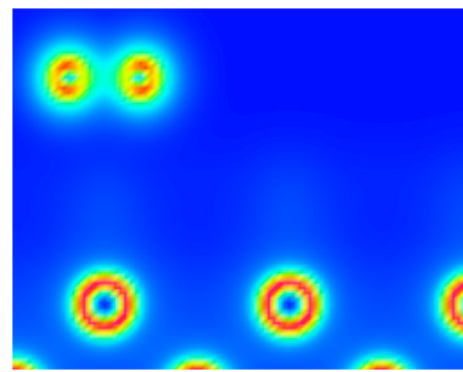
Figure 22: Orthogonal view of figure 21 is shown to see the bonding between the two oxygen atoms.

Now that the DOS plots have been considered one might take a cut of the charge density plot of the situations where the molecule is in the energy minimum. The charge densities of the situations are shown in figures 19-21. In the figures, it can be seen that the charge density between the molecule and the surface atoms is not increased. This indicates, that there is no bonding between the surface and the molecule in either case. In both cases the bonding is obvious between the oxygen atoms. This can be fairly said by the increased charge density between the oxygen atoms. This also confirms our impression from the DOS figures that the oxygen atoms above the surface bond to each other and the surface does not effect the molecule much. In fact when looking at the charge density figures one

gets the impression that no charge transfer between the molecule and the surface happens in the second case. In the first case, on the other hand, there seems to be some small amount of charge between the molecule and the nearest neighboring coppers as seen in figure 19. Also, in the second case, the molecule is closer to the surface, and therefore this result is not very surprising.
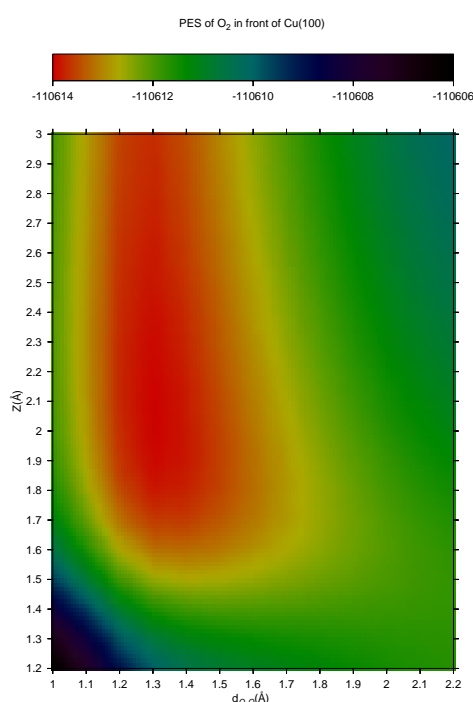
5.4.3   Molecular oxygen on top of the rise
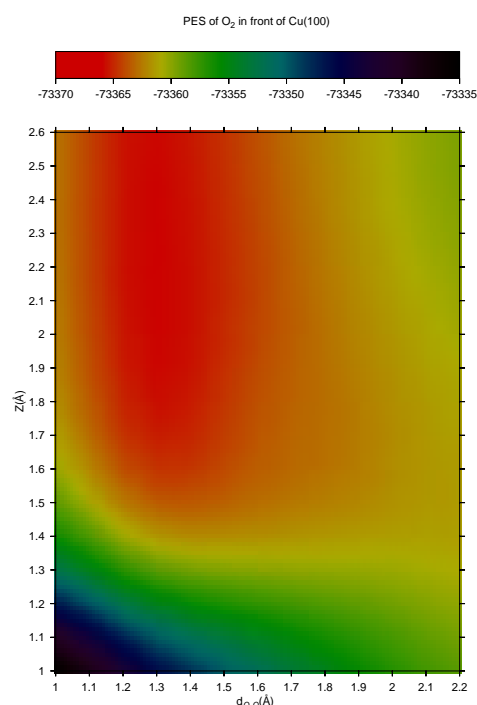

Figure 23: Potential energy surface for O_2 in case 3.

Figure 24: Potential energy surface for O_2 in case 4.

Next, we calculated the PES for situations 3 and 4, which are shown in figures 23 and 24. These were done using the SIESTA method. This means that the DOS figures are not comparable with the figures drawn from the VASP calculations as the units of these figures do not match. Judging by the figures the PES plots for the situations in the two cases differ remarkably from each other, even though their geometric sites are quite similar. The only difference between these two sites are that the case 4 is rotated $45°$ in the direction of the surface, as seen in figure 10. In the PES plots it can be seen that in case 4 the molecule

is more willing to break than in case 3. Although, one can not say that case 4 would be a trajectory that breaks the molecule. The molecule still needs external energy to break as seen in figure 24 as it has a minimum at the entrance channel. Perhaps, this barrier could be overcome with the assistance of thermal energy. As in the previous two cases these PES plots must be tested using MD, because, again, these are just two dimensional cuts of the real potential energy surface and the ions are not relaxed during the different phases
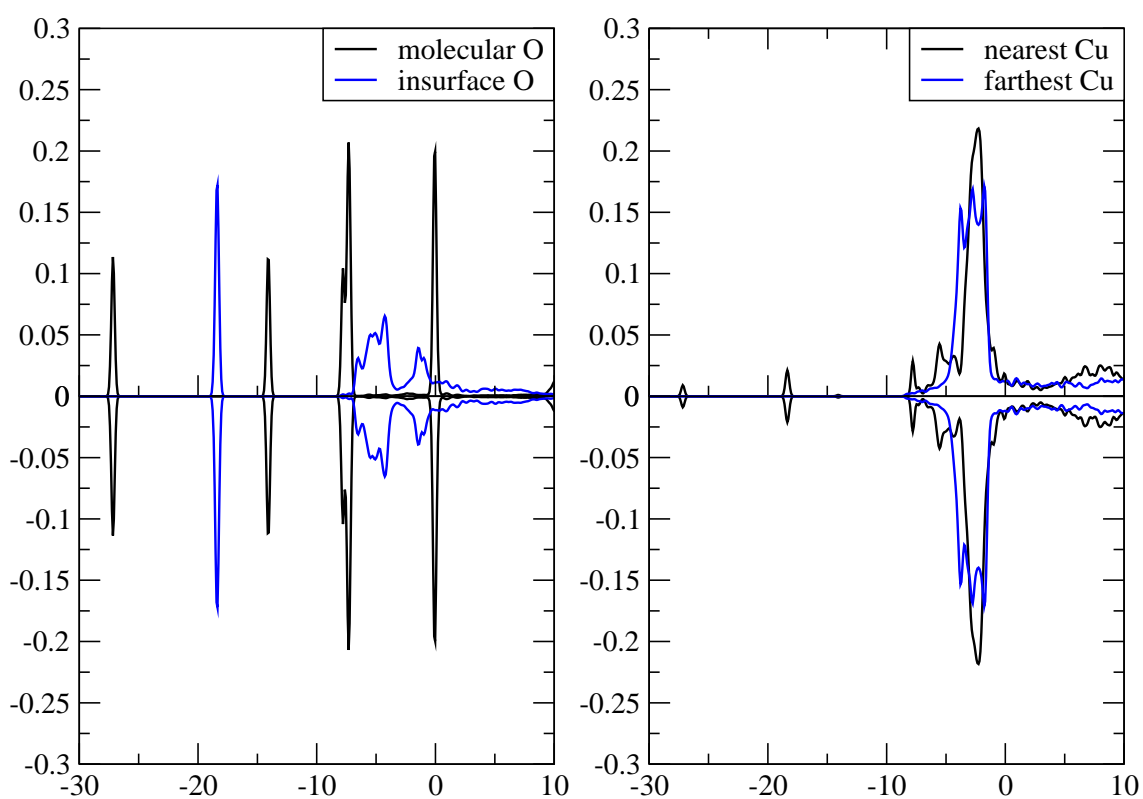
Figure 25: Density of states of case 3. Upper part of the figure presents the spin up and lower part presents the spin down.

Then, one has to take the DOS in the energy minima into consideration. The DOS plots for the situations are presented in figures 25 and 26. In figure 25 it can be seen, that the molecule stays in molecular form as the molecular spikes exist in the DOS plot. Also, the spin down and spin up densities have moved with respect to each other in such a
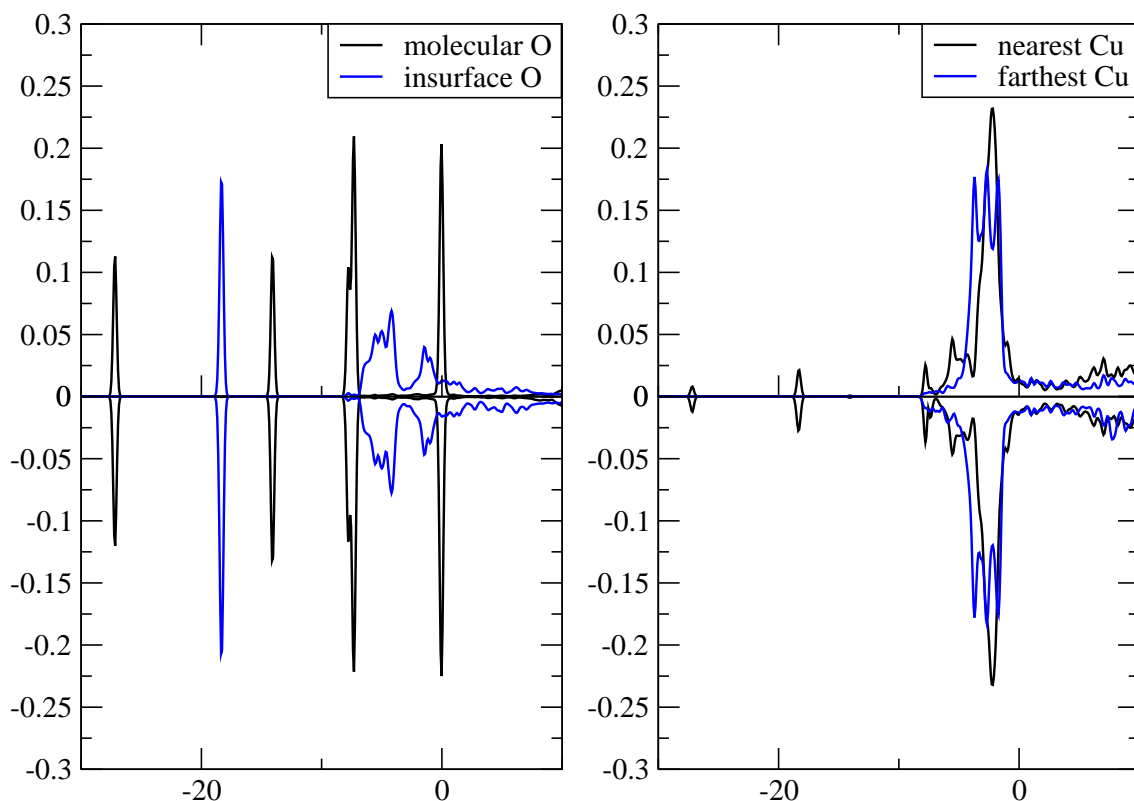
Figure 26: Density of states of case 4. Upper part of the figure presents spin up and lower part presents spin down.

way, that the spikes in both directions are at the same places and therefore the DOS is symmetric. When looking at the copper closest to the molecule there exist a lot of states near the Fermi level and some states much lower at energies about -37 eV where some of the molecular spikes of the oxygen seems to be. This indicates antibonding between the nearest copper and the molecule. When comparing these two situations there are some states for the insurface oxygen which have moved to bonding state of the molecular oxygen. The main impression that both of these figures give, is that there is not that much difference in the densities between these two situations. So the reason for the PES figures being so different is not due to an electronic effect.

Finally, the charge densities of the both situations are drawn to see if there is some bonding and charge transfer between the surface and the molecule. The charge densities for
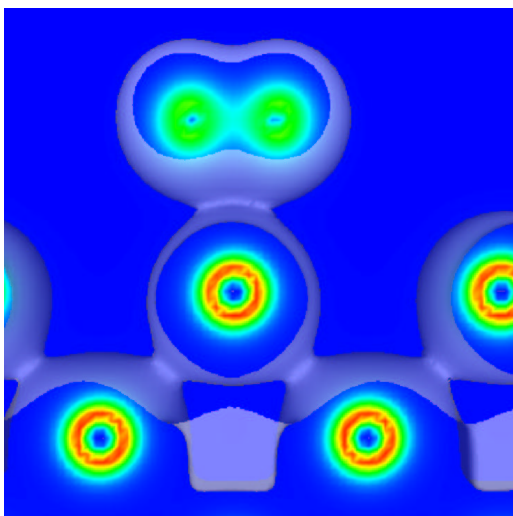
38

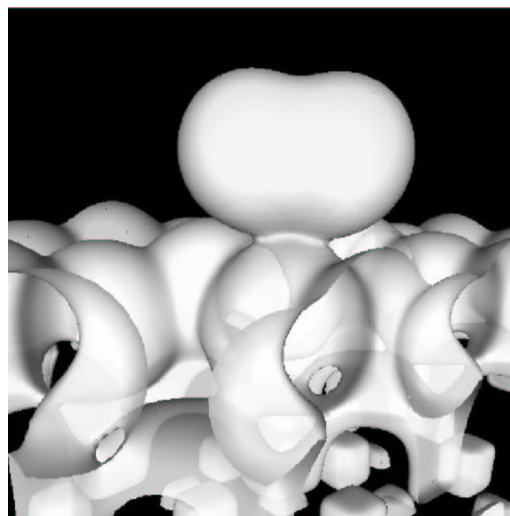Figure 27: Charge density plot in case 3.   Figure 28: Charge density plot in case 4.

these cases are shown in figures 27 and 28. These are, of course, carefully chosen two dimensional cuts of the actual three dimensional density. In both of these figures it can be seen that there is some small amount of charge between the surface and the molecule. This indicates that there is some sort of charge transfer between the molecule and the surface. This transfer is, however, so small that one can not say that these two objects are bonding with each other. In the figures, it is obvious, though, that the molecular bonding between the two oxygen atoms remains. It is quite surprising that the charge densities in cases 3 and 4 differ only that little, because the PES plot of the latter case showed only a weak minimum in the entrance channel. This might be explained by the fact that the minimum is at the same height and therefore the electron density between the surface and the molecule is of about the same magnitude. The difference in the PES plots might be explained by the difference in the geometry of these situations. In case 3 the oxygen atoms in the molecule are far away from the insurface oxygen atoms, whereas in case 4 the oxygen atoms in the molecule are closer to the insurface oxygens. On the other hand, there is the issue about four fold hollow site being the most favorable site on the clean copper (100) surface, therefore one automatically suspects that the geometry for the case 3 would be more likely to be the breaking trajectory. This is, however, not the case, as seen in the PES plots. When the same trajectories for the clean and reconstructed surface are compared the splitting trajectory seems to be the one where the oxygen atoms are placed so, that the atoms would land in the bridge sites rather than in the hollow sites.

5.4.4 Molecule on the edge of the rise

In this case the molecule was in a position which is marked with number 5 in figure 10. The potential energy surface for this case is shown in figure 29. In the figure it can be seen that there exists energy minimum at 1.7 Å above the surface. This indicates, that the molecule does not like to break but, as in all the cases for the reconstructed surface, it stays as a molecule if no steering effect takes place. If this case is compared to the other ones, it can be fairly said that the minimum in this case is much stronger than in any previous ones; Nearly a 10 eV barrier stops the molecule from breaking. Still if the molecule would gain such a high kinetic energy, even in this case, it probably would break. This also gives support for the experiments where the sticking coefficient raises as the kinetic energy of the molecule rises.
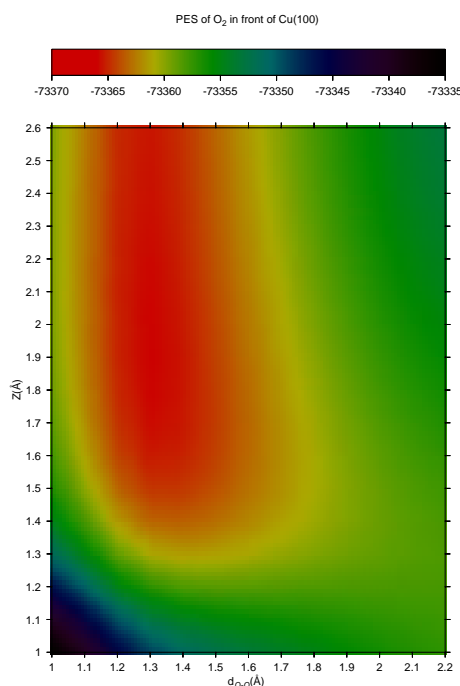

Figure 29: A cut of the potential energy surface in case 5. A quite strong minimum exists straight above the surface.

At the DOS plot drawn in figure 30, there seems to be some small hybridization between the states of the molecule and the Cu atom straight below the molecule. This would indicate a weak chemisorped state for the molecule. As in the PES plot this shows that
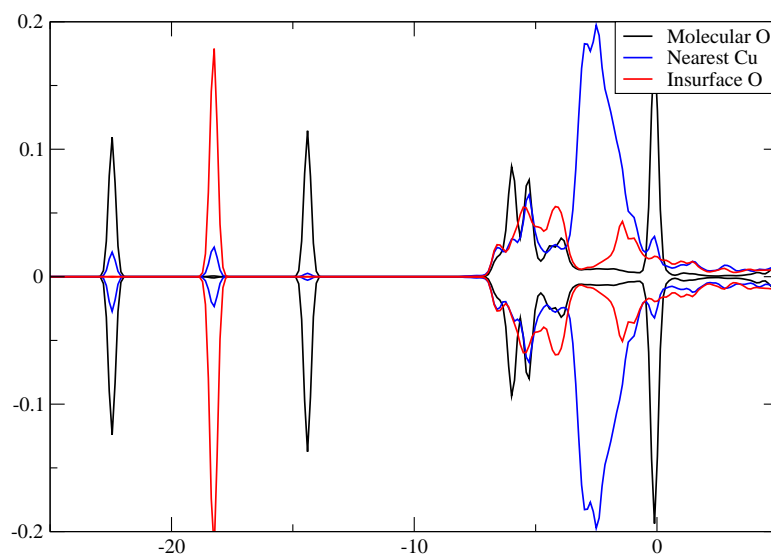
Figure 30: DOS in case 5 showing small hybridization between Cu and oxygen atom in the molecule.
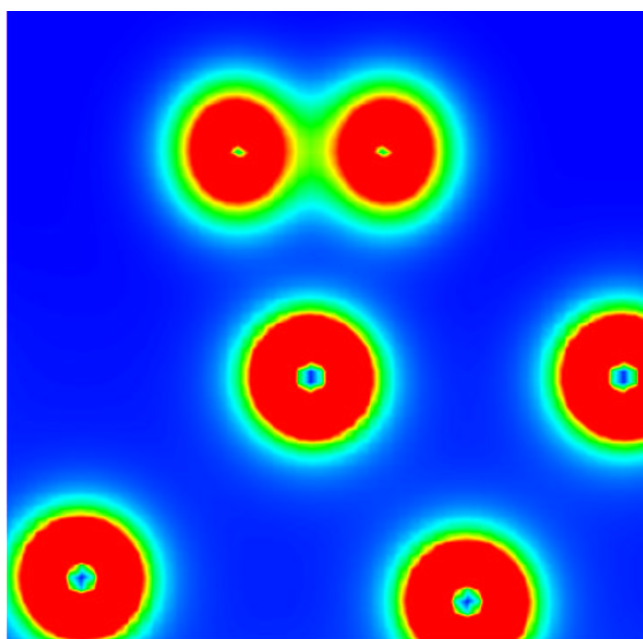

Figure 31: Charge density between the molecule and the nearest copper atoms in case 5. Notice the lowered amount of charge between the oxygen atoms, and the increased amount of charge between the molecule and the copper atom below.

the molecule will not stay at this site as there is not much barrier above the molecule and therefore it can move away from this site with its kinetic energy. Therefore it can be said that this, as all the other sites for the reconstucted surface so far, is not very reactive.

Still, one might take a look at the charge density of this situation, that is shown in figure 31. Again, as in all the previous cases for the reconstucted surface, the charge density shows a small charge transfer between the surface and the molecule, but nothing worth considering. The amount of charge is increased between the surface and the molecule, yet not a clear bond is formed. This most likely indicates that the molecule will not stay in this minimum, but will be steered to some other place on the surface. The distance between the oxygen atoms at the energy minimum is about 1.4 Å.

5.4.5 O_2 above the missing row

In this case the molecule was located above the missing row, as shown in the chematic figure 10, case number six. In this case the molecule would not physically fit inside the missing row. Using the PES approach we get the plot shown in figure 32. As seen in the figure, again the molecule will not break unless it gets a ridiculously high energy. This amount of kinetic energy in this scale is only a matter of academic discussion and not in any way realistic. If the molecule would gain such a high kinetic energy and collide in to the surface, the surface would most likely face very huge deformation and the case would not remain the same. In the PES plot there is a high barrier for the molecule to get away from the surface (about 5 eV). This indicates a molecularly chemisorbed state.

Let us consider the DOS for this case to see if our suspicion about the chemisorbed state is a correct one. Clearly there is not much hybridization between the nearest copper and the molecule. Only a small hybridization is seen in the states lower in the energy. Near the Fermi level there is not much happening. On the other hand, as it should, there is a very strong hybridization between the insurface oxygen and the nearest copper and the bond between the atoms is very clear. To see the bonding more clearly, again, we must take the electron charge density into consideration. In figure 34 is shown a two dimensional charge density plot for case six. When comparing this figure, for example, to the one for the previous case, there exists much more charge between the atoms in the molecule
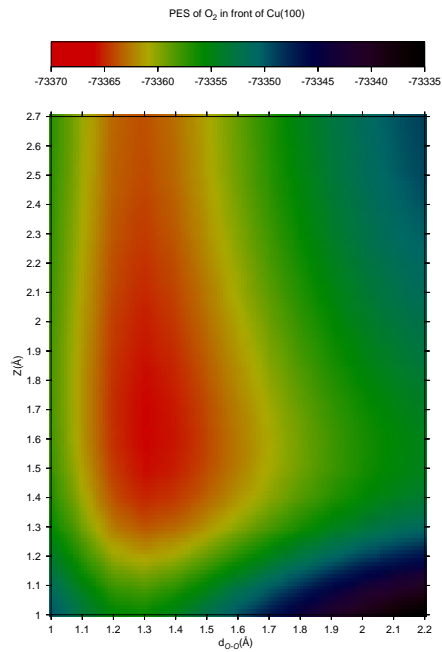
Figure 32: Potential energy surface for the case six showing an intense minimum. This figure leads us to think that this might be a molecularly chemisorped state.
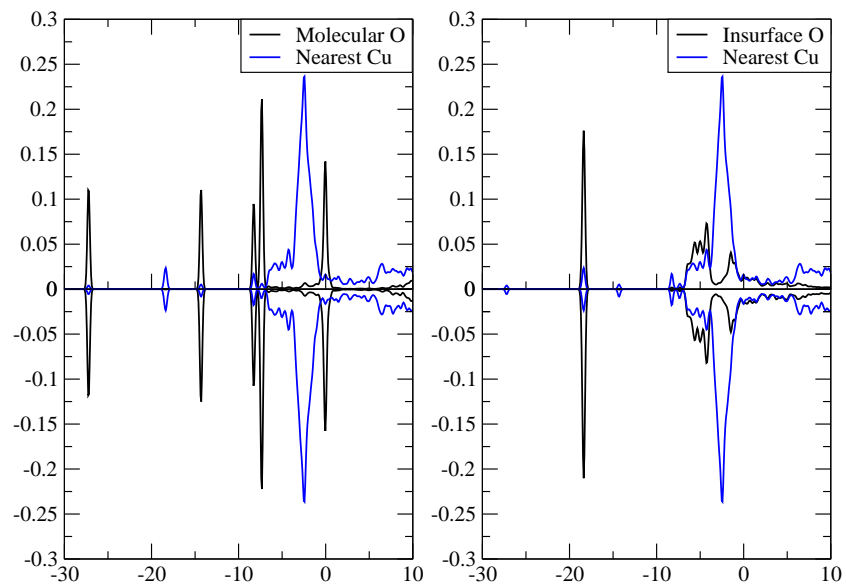

Figure 33: DOS for the molecule and the nearest copper and oxygen. Negative side of the vertical axis corresponds to the spin down, and positive corresponds to the spin up.
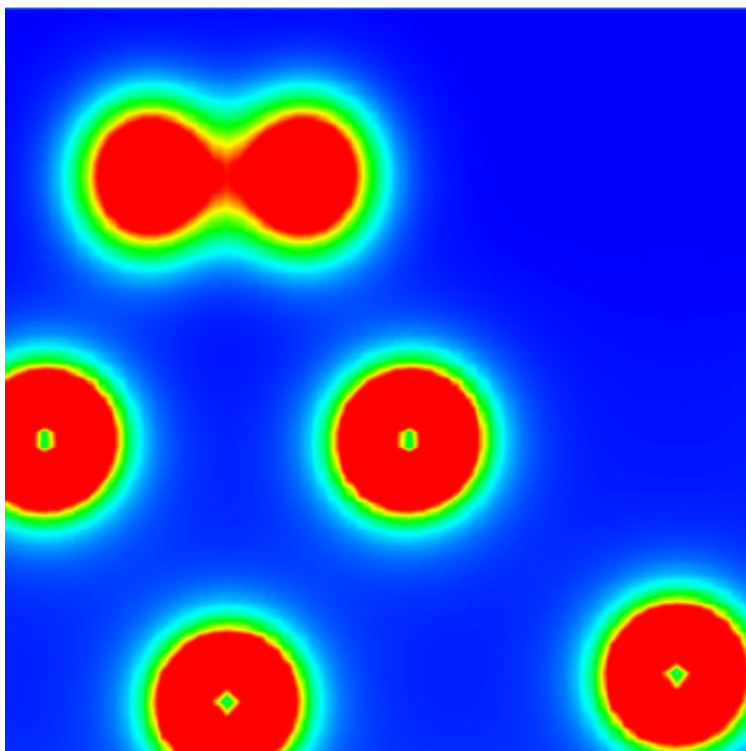
Figure 34: Electron charge density for case 6. Notice the increased density between the atoms in the molecule. Also, there is small charge transfer between the molecule and the surface.

than in the previous case. The distance between the oxygen atoms at the energy minimum is about 1.2 Å, which is somewhat shorter than in the previous case. This can partially explain the difference in the charge density plots. If the molecule does not confront any steering effect this site could well be a molecularly chemisorbed site. This should, of course, be confirmed using molecular dynamics.

5.4.6 O_2 on the reconstructed surface using MD

In figure 35 are shown the cases, where MD was applied for the precovered surface. These cases were selected because of their interesting properties seen in the PES plot or to do comparison between the clean and the precovered surfaces. Unfortunately there was not enough time, physical nor cpu, to do MD for all the abovementioned cases.
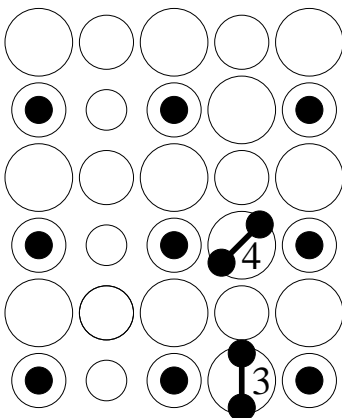
Figure 35: Schematic figure that shows which of the previous cases were calculated using MD for the oxygen precovered surface.

In both of these cases the oxygen molecule did not move as it was expected to according to the PES calculations shown in the previous chapters. In case 3 we used only 50 meV kinetic energy for the molecule and the surface temperature was set to 300 K. The molecule bounced of the copper atom straight below it and steered away from the site even though the PES showed a very clear minimum above the surface. After bouncing from the copper atom, it started to rotate vertically and ended up in an almost vertical position between the sites 4 and 3 with bond length of 1.292 Å, which is only a bit longer than the bonding distance of a free molecule.

In case 4 the deformation of the surface is much more considerable than in the previous case. As the molecule approaches the surface, the copper atom straight below goes deeper in the surface getting out of the molecules way. This calculation is not entirely finished and therefore it is hard to say where the molecule finally ends up.

6   Conclusions

6.1   Reliability of the PES calculations

PES calculations can not be trusted alone and MD should always be used to confirm the trajectories. This is because the PES calculations performed traditionally are missing the change in the potential energy surface during this relaxation and therefore partially generating the steering effect. The change in the potential energy surface is caused by the mobility of the surface atoms that are affected by the proximity of the molecule. To improve the results of the PES calculations the surface must be allowed to relax during the calculation. This is not as simple a task as it sounds, because this makes an enormous cost in cpu time. Approximately ten conventional PES plots can be calculated, using the traditional method, per each PES where the surface has been let to relax between the steps. Even then the results would be at least questionable as the weight of the molecule would be approximated to be very high. The conventional PES calculations can be used as calculations which give direction about where to start the more time consuming calculations, for example, MD calculations. The total energy minimum of the PES calculations seems to give indication on the height, at which above the surface something starts to happen. For example in the MD calculation for the reconstructed surface at the same height where the minimum of the PES calculation was, the molecule turned in such a way, that the molecular axis was perpendicular to the surface. As seen throughout the Results section the construction of even a two dimensional cut of the potential energy surface is very hard if not impossible. New ideas for this task are definitely needed.

Also, one has to bear in mind, that the DFT itself is not perfect. It does not take into account the nonadiabatic effects, such as the Born couplings of different electronic states or the Van der Waals interaction, and therefore even in the best case we might be missing something. Nonadiabatic effects can be taken into account theoretically, for example, by building a model, as Helmann *et al.* [30] did for Al(111) surface. Another method, which can be applied for this kind of problem is the Time Dependent Density Functional Theory (TDDFT) which is implemented in, for example, the Octopus [31] code.

6.2   O$_2$ adsorption to the clean copper surface

In both cases considered here the O$_2$ would adsorb in molecular state and the bonding between the oxygen atoms would not break. This is one calculation that confirms that the PES calculation is missing something here. The PES calculated earlier shows clearly and without a doubt a trajectory that should break the molecule. When the molecule is sent along with these two trajectories it is supposed to break, but it seems that if the kinetic energy of the molecule is too small, the molecule will encounter some sort of steering effect and get steered as a molecule to one of the four fold hollow sites, that are closest to the copper atom, which they collided into. If the kinetic energy of the molecule is large enough, the molecule will break and the individual atoms will adsorb to the four fold hollow sites residing in both sides of the copper atom. There is a need of nudged elastic band (NEB) method [32] to be used to calculate the barriers for the oxygen atoms to diffuse or jump away from this molecularly adsorped state in order to make a Monte Carlo model, which is needed to get deeper in this matter of oxidation of copper.

6.3   O$_2$ adsorption to the O precovered copper surface

As in experimental studies, these calculations also clearly showed that there are not that many sites where the oxygen might adsorp in the precovered surface. After the reconstruction the sticking coefficient gets lower and this is also consistent with the experimental results. The oxidation process still continues, but at a lower rate. In this case also the Monte Carlo model might be able to tell us some more details about how this actually happens. By these calculations we can, however, say that there are much less dissociative trajectories in the reconstructed surface than there are in the clean surface. In fact, we did not find any dissociative trajectory from this surface. On the other hand, we found a few potential molecular adsorption sites, which still need to be confirmed using MD.

REFERENCES

[1] M. Kittel, M. Polcik, R. Terborg, J.-T. Hoeft, P. Baumgärtel, A. M. Bradshaw, R. L. Toomes, J.-H. Kang, D. P. Woodruff, M. Pascal, C. L. A. Lamont, E. Rotenberg, Surf. Sci. **470**, 311 (2000).

[2] S. Stolbov, T. S. Rahman, J. Chem. Phys. **117** 8523 (2002).

[3] N. Cabrera, and N. F. Mott, Rep. Prog. Phys. **12** 163 (1948).

[4] G. Zhou, and J. C. Yang, Phys. Rev. Lett. **89**, 106101 (2002).

[5] J. C. Yang, M. Yeadon, B. Kolasa, And J.M. Gibson, Appl. Phys. Lett **70**, 3522 (1997).

[6] A. Puisto, H. Pitkänen, and M. Alatalo, unpublished.

[7] Y. Xu and M. Mavrikakis, Surf. Sci. **494**, 131 (2001).

[8] H. T. Pitkänen, private communication (2003).

[9] S. Stolbov and T. S. Rahman, Phys. Rev. Lett. **89**, 116101 (2002).

[10] I. K. Robinson and E. Vlieg, Phys. Rev. B **42**, 6954 (1990).

[11] M. Wuttig, R. Franchy, H Ibach, Surf. Sci. **213**, 103 (1989).

[12] C. H. Wöll, R. J. Wilson and S. Chiang, Phys Rev. B **42**, 11926 (1990).

[13] P.Hohenberg and W. Kohn, Phys Rev. B **136**, 864 (1964).

[14] W. Kohn and L. J. Sham, Phys. Rev. A **140**, 1133 (1965).

[15] D. Vanderbilt, Phys. Rev. B **41**, 7892 (1990).

[16] G. Kresse and J. Hafner, J. Phys.: Condens. Matter **6**, 8245 (1994).

[17] P. Ordejón, E. Artacho and J. M. Soler, Phys. Rev. B (Rapid Comm.) **53**, R10441 (1996).

[18] J. M. Soler, E. Artacho, J. D. Gale, A. García, J. Junquera, P. Ordejón and D. Sánchez-Portal, J. Phys.: Condens. Matter **14**, 2745 (2002).

[19] D. R. Hamann, M. Schlüter, and C. Chiang, Phys. Rev. Lett. **42**, 1494 (1979).

[20] G. B. Bachelet, D. R. Hamann, and M. Schlüter, Phys. Rev. B **26**, 4199 (1982).

[21] N. Troullier, J.L. Martins Phys. Rev. B **43**, 1993 (1991).

[22] L. Laaksonen, J. Mol. Graph. **10**, 33 (1992).

[23] D. L. Bergman, L. Laaksonen, and A. Laaksonen, J. Mol. Graph. Model. **15**, 301 (1997).

[24] L. E. Sutton (ed.), Supplement 1956-1959, Chemical Society, London UK, Special publication **18** (1965).

[25] H. J. Monkhorst and J. D. Pack, Phys. Rev. B **13**, 5188 (1976).

[26] N.Chetty, M. Weinert, T. S. Rahman, J. W. Davenport, Phys. Rev. B **52**, 6313 (1995).

[27] M. Alatalo, S. Jaatinen, P. Salo, and K. Laasonen, unpublished.

[28] D. M. Lind, F. B. Dunning, and G. K. Walters, Phys. Rev. B **35**, 9037 (1987).

[29] Th. Rodach, K.-P. Bohnen, and K. M. Ho, Surf. Sci. **286**, 66 (1993).

[30] A. Hellman, B. Razaznejad, Y. Yourdshahyan, H. Ternow, I. Zoric, B. I. Lundqvist, Surf. Sci. **532-535**, 126 (2003).

[31] M. A. L. Marques, A. Castro, G. F. Bertsch, A. Rubio, CPC **151**, 60 (2003).

[32] G. Mills, H. Jonsson and G. K. Schenter, Surf. Sci. **324**, 305 (1995).